*Article*

# Modulation of the Cardiac Myocyte Action Potential by the Magnesium-Sensitive TRPM6 and TRPM7-like Current

Asfree Gwanyanya [1,2], Inga Andriulė [3], Bogdan M. Istrate [1], Farjana Easmin [1], Kanigula Mubagwa [1,4] and Regina Mačianskienė [3,*]

1   Department of Cardiovascular Sciences, KU Leuven, 3000 Leuven, Belgium; asfree.gwanyanya@uct.ac.za (A.G.); istratem.bogdan@yahoo.com (B.M.I.); feasmin87@gmail.com (F.E.); kanigula.mubagwa@kuleuven.be (K.M.)
2   Department of Human Biology, University of Cape Town, Cape Town 7925, South Africa
3   Institute of Cardiology, Lithuanian University of Health Sciences, 50103 Kaunas, Lithuania; inga.andriule@lsmuni.lt
4   Department of Basic Sciences, Faculty of Medicine, Université Catholique de Bukavu, Bukavu, Congo
*   Correspondence: regina.macianskiene@lsmuni.lt

**Abstract:** The cardiac $Mg^{2+}$-sensitive, TRPM6, and TRPM7-like channels remain undefined, especially with the uncertainty regarding TRPM6 expression in cardiomyocytes. Additionally, their contribution to the cardiac action potential (AP) profile is unclear. Immunofluorescence assays showed the expression of the TRPM6 and TRPM7 proteins in isolated pig atrial and ventricular cardiomyocytes, of which the expression was modulated by incubation in extracellular divalent cation-free conditions. In patch clamp studies of cells dialyzed with solutions containing zero intracellular $Mg^{2+}$ concentration ($[Mg^{2+}]_i$) to activate the $Mg^{2+}$-sensitive channels, raising extracellular $[Mg^{2+}]$ ($[Mg^{2+}]_o$) from the 0.9-mM baseline to 7.2 mM prolonged the AP duration (APD). In contrast, no such effect was observed in cells dialyzed with physiological $[Mg^{2+}]_i$. Under voltage clamp, in cells dialyzed with zero $[Mg^{2+}]_i$, depolarizing ramps induced an outward-rectifying current, which was suppressed by raising $[Mg^{2+}]_o$ and was absent in cells dialyzed with physiological $[Mg^{2+}]_i$. In cells dialyzed with physiological $[Mg^{2+}]_i$, raising $[Mg^{2+}]_o$ decreased the L-type $Ca^{2+}$ current and the total delayed-rectifier current but had no effect on the APD. These results suggest a co-expression of the TRPM6 and TRPM7 proteins in cardiomyocytes, which are therefore the molecular candidates for the native cardiac $Mg^{2+}$-sensitive channels, and also suggest that the cardiac $Mg^{2+}$-sensitive current shortens the APD, with potential implications in arrhythmogenesis.

**Keywords:** TRPM6; TRPM7; ion channel; action potential; cardiac; magnesium; myocyte

## 1. Introduction

The cardiac cation channels involved in electrical activity and ion homeostasis include well-known ion-selective channels, as well as ion nonselective channels. Apart from the $Na^+$- and $K^+$-permeable pacemaker or funny ($I_f$) channels [1], not many nonselective cardiac cation channels have been fully characterized; hence, their molecular identities remain uncertain. During the past two decades, there has been a growing interest in transient receptor potential (TRP) proteins as molecular candidates for native cation nonselective channels, including those found in the heart [2]. TRP channels are a large superfamily of proteins expressed in several tissues where they are involved in diverse signaling processes and in disease [3]. Among the various TRP channels expressed in the cardiovascular system, canonical (e.g., TRPC1 and C3–C7), melastatin (e.g., TRPM4 and M7), vanilloid (e.g., TRPV1 and V2), and polycystin (e.g., TRPP1/2) channels are present in the heart and are implicated in the physiological functions and in cardiac abnormalities such as arrhythmogenesis and heart failure [4,5]. The role of cardiac TRP channels has been explored in fibroblasts and in pacemaker cells (see reference [3]) but much less in cardiomyocytes. The few TRPs

that have been electrophysiologically explored in cardiac myocytes include TRPC1 [6], TRPC3/6/7 [7,8], TRPV4 [9], TRPM4 [10], TRPM7 [11,12], and TRPP1/2 [13].

We have previously characterized cardiac $Mg^{2+}$-sensitive channels [14,15] with biophysical properties similar to those of the heterologous TRPM6 and TRPM7 channels, both of which are involved in the homeostasis of $Mg^{2+}$ and other divalent cations [16–20]. Like the heterologously expressed TRPM6 and TRPM7 channels, the cardiomyocyte TRPM6- and TRPM7-like channels are typically activated by low intracellular $Mg^{2+}$ concentration ($[Mg^{2+}]_i$) conditions and conduct small inward currents carried by divalent cations and large outward currents carried by monovalent cations. These cardiomyocyte $Mg^{2+}$-sensitive channels have been detected in various species, including humans, rats, pigs, guinea pigs, and mice. However, the nature of the proteins underlying the cardiac TRPM6- and TRPM7-like currents and the functional consequences of their cation fluxes have remained unclear.

Whereas TRPM7 protein expression has been systematically detected in cardiac tissues or cells, until recently, information regarding the TRPM6 channel protein expression in the heart has remained scant and has concerned only the right atrium [21]. However, very recent data on human atrial/ventricular cardiomyocytes and tissues has highlighted the co-expression of TRPM6 and TRPM7 in cardiomyocytes from all chamber walls of the human heart [22]. As far as function is concerned, we have previously shown the cardiac $Mg^{2+}$-sensitive channels to be permeable to $Ca^{2+}$ and $Mg^{2+}$ [15] and proposed that, at the resting membrane potential, the inward flow of divalent cations into cells through the channels could have an effect on the intracellular concentrations of the divalent cations (see reference [23]). On the other hand, the contribution of the TRPM6- and TRPM7-like currents to the cardiomyocyte electrical activity is unknown. The possibility that monovalent cation effluxes through $Mg^{2+}$-sensitive channels at positive potentials could contribute to action potentials has not been tested.

Here, we investigated the expression profile of TRPM6 and TRPM7 proteins in pig cardiac myocytes, as well as the role of the $Mg^{2+}$-sensitive, TRPM6-, and TRPM7-like currents on the cardiac action potential.

## 2. Results

### 2.1. Expression of TRPM6 and TRPM7 in Cardiac Myocytes

To show the presence of TRPM6 and TRPM7 proteins, we used the immunostaining of atrial and ventricular cardiomyocytes, performed after 2 h of cell isolation. Figure 1A–D shows confocal images of pig cardiomyocytes co-stained for the nucleus (blue), for either TRPM7 or TRPM6 protein (green), and for the F-actin-cytoskeleton (red), whereas Figure 1E shows a negative control (cardiomyocyte incubated in conditions similar to those of Figure 1A–D but with no primary antibody added in the incubation medium). All the cardiomyocytes displayed staining with antibodies for TRPM6 and TRPM7. Figure 1F shows the quantification of the immunodetected fluorescence of TRPM7 (left panel) and TRPM6 (right panel) in the four cardiac chamber walls: left atrium (LA), right atrium (RA), left ventricle (LV), and right ventricle (RV). Of note was the multinucleated nature of the cells, as previously noted for pig cardiomyocytes [24].

We found that the measured level of expression of the TRPM6 and TRPM7 proteins was influenced by the cell incubation conditions, such as the presence and absence of extracellular divalent cations. The immunofluorescence level of both channel proteins in the cardiomyocytes from all the cardiac chamber walls was significantly higher following cell incubation in divalent cation-containing (DV) extracellular conditions vs. incubation in divalent cation-free (DVF) conditions (see Table 1). In addition, the expression was also increased when incubating cells for a longer period before cell fixation and exposure to the primary antibodies. Figure 2 shows that the mean fluorescence levels for the immunodetected TRPM6 and TRPM7 were significantly increased in LV cardiomyocytes kept for 12 h in solutions with (Figure 2A,B) or without (Figure 2C,D) divalent cations. TRPM7 increased from $0.087 \pm 0.0013$ a.u. to $0.133 \pm 0.0011$ a.u., $n = 3$–23, $p < 0.001$ in the

DV solutions and from $0.065 \pm 0.0009$ a.u. to $0.112 \pm 0.0006$ a.u., $n = 4$–25, $p < 0.001$ in the DVF solutions. Under the same experimental conditions, the TRPM6 immunofluorescence increased from $0.029 \pm 0.0015$ a.u. to $0.050 \pm 0.0012$ a.u., $n = 3$–24, $p < 0.001$ and from $0.020 \pm 0.0006$ a.u. to $0.040 \pm 0.0009$ a.u., $n = 7$–21, $p < 0.001$ in the DV and DVF solutions, respectively. Qualitatively similar changes could be detected in the cardiomyocytes from the other cardiac chamber walls when incubated for 12 h (not illustrated).
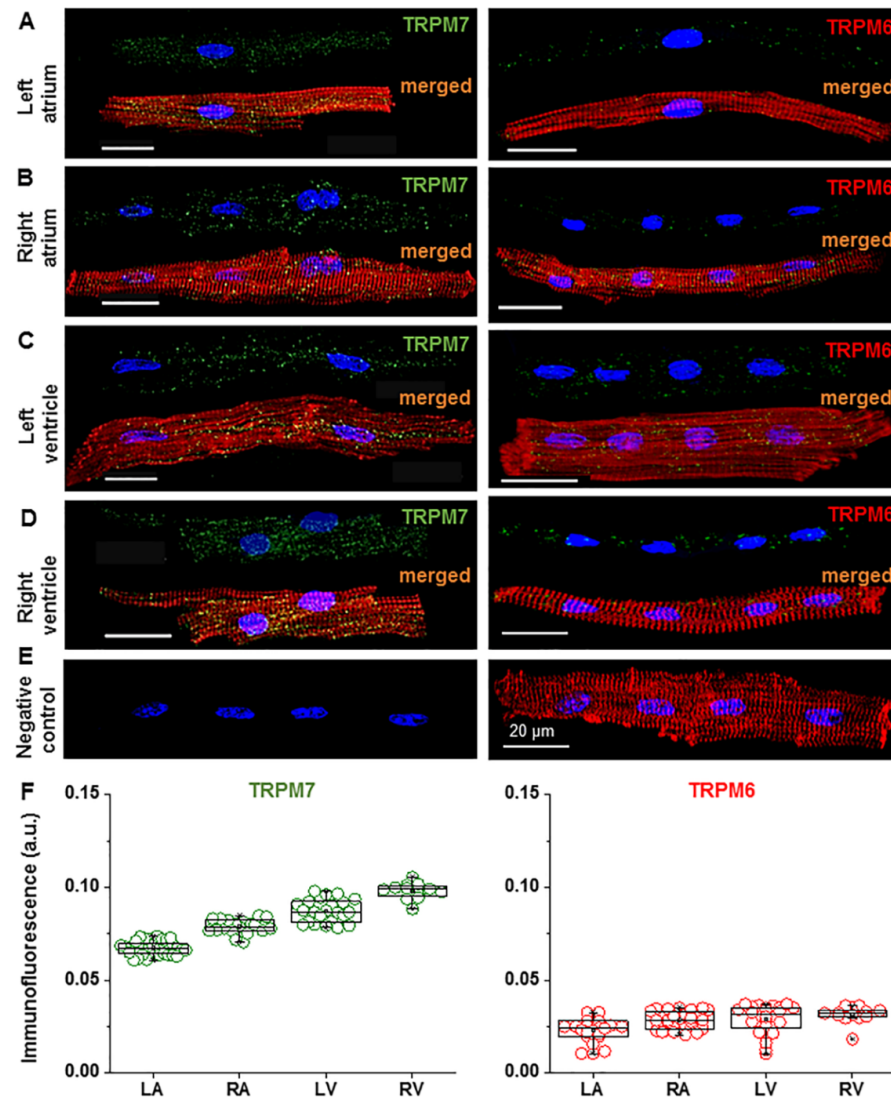


**Figure 1.** Immunofluorescence images suggesting the presence of TRPM6 and TRPM7 proteins in pig cardiomyocytes from different cardiac chamber walls. (**A–D**) Immunofluorescence of TRPM7 (left) and TRPM6 (right) in the left atrium (LA), right atrium (RA), left ventricle (LV), and right ventricle (RV) cardiomyocytes when using Alexa Fluor 488 for the TRPM7 and TRPM6 proteins (stained in green), Alexa Fluor 546 for the F-actin cytoskeleton (stained in red), and Hoechst 33342 for the nuclei (stained in blue). Scale bars indicate 20 μm. (**E**) Example of a negative control, where the primary antibody for TRPM6 and/or TRPM7 is not added, but the cardiomyocyte was subjected to Hoechst 33342 and Alexa Fluor 546. Under such conditions, only immunofluorescence of the nuclei (stained in blue) and F actin cytoskeleton (stained in red) is detected. Note: same cardiomyocyte in the left and right (merged image) panels (**F**) Quantification of the staining intensity of the immunodetected fluorescence of TRPM7 and TRPM6 in the four cardiac chamber walls: LA, RA, LV, and RV. The mean data is provided in arbitrary units (a.u.) (see Table 1). A blinded study design (with the origin or treatment of cells unknown to the investigator) was used for the detection of immunofluorescence during the various experimental conditions.

**Table 1.** Immunofluorescence signals of the TRPM7 and TRPM6 proteins in pig hearts.

| Heart Chamber | TRPM7 Signal (a.u.) | | TRPM6 Signal (a.u.) | |
|---|---|---|---|---|
| | DV | DVF | DV | DVF |
| LA | $0.067 \pm 0.0006$ $n = 37$ | $0.053 \pm 0.0009$ # $n = 13$ | $0.023 \pm 0.0013$ $n = 18$ | $0.016 \pm 0.0014$ # $n = 20$ |
| RA | $0.079 \pm 0.0009$ $n = 21$ | $0.059 \pm 0.0010$ # $n = 5$ | $0.029 \pm 0.0008$ $n = 32$ | $0.018 \pm 0.0011$ # $n = 4$ |
| LV | $0.087 \pm 0.0013$ $n = 23$ | $0.065 \pm 0.0009$ # $n = 25$ | $0.029 \pm 0.0015$ $n = 24$ | $0.020 \pm 0.0006$ # $n = 21$ |
| RV | $0.098 \pm 0.0013$ $n = 12$ | $0.076 \pm 0.0016$ # $n = 5$ | $0.032 \pm 0.0012$ $n = 14$ | $0.025 \pm 0.0020$ # $n = 3$ |

TRPM7 and TRPM6—transient receptor potential melastatin type 7 and 6 channels, LA—left atrium, RA—right atrium, LV—left ventricle, RV—right ventricle, DV—extracellular divalent cations, DVF—extracellular divalent cation-free, *n*—number of cells, a.u.—arbitrary unit, and #—$p < 0.001$ for DV vs. DVF.
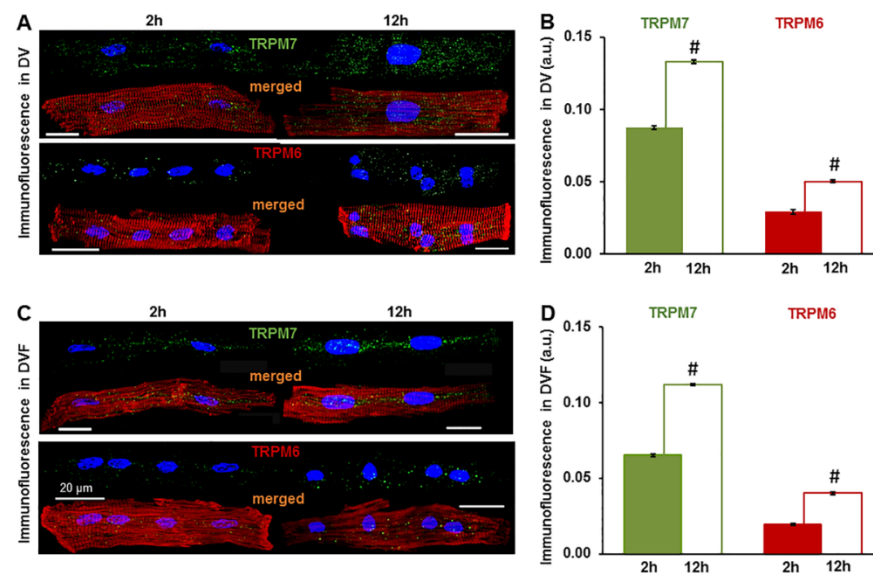


**Figure 2.** Comparison of the expression of TRPM6 and TRPM7 in left ventricular cardiomyocytes incubated for 2 h vs. 12 h in extracellular solutions with (**A**,**B**) and without (**C**,**D**) divalent cations (DV and DVF, respectively). (**A**,**C**) The cardiomyocytes were fixed after 2 h (filled columns) or 12 h (unfilled columns) of cell isolation: Alexa Fluor 488 for the TRPM7 and TRPM6 proteins (stained in green), Alexa Fluor 546 for the F-actin cytoskeleton (stained in red), and Hoechst 33342 for the nuclei (stained in blue). Scale bars indicate 20 μm. (**B**,**D**) Quantification of the intensity of the fluorescence expressed in arbitrary units (a.u.). # $p < 0.001$ expression after 12 h vs. 2 h of cardiomyocyte incubation.

## 2.2. Impact of $Mg^{2+}$-Sensitive Currents on the Action Potential

To examine the role of $Mg^{2+}$-sensitive currents on the electrical activity of cardiac myocytes, we recorded the total currents using a whole-cell voltage clamp, as well as the resting and action potentials using the current clamp. The cells were internally dialyzed and extracellularly perfused with solutions known to activate or inhibit the currents. The cells were internally dialyzed with either physiological levels of free intracellular $[Mg^{2+}]$ ($[Mg^{2+}]_i = 0.8$ mM) or with the $Mg^{2+}$-free solution ($[Mg^{2+}]_i \approx 0$ mM). The latter condition is known to cause a progressive activation of $Mg^{2+}$-sensitive channels with time by removing the inhibition exerted by intracellular $Mg^{2+}$ [15]. The cells were also extracellularly perfused with either physiological levels of $[Mg^{2+}]$ ($[Mg^{2+}]_o = 0.9$ mM) or with high $Mg^{2+}$ ($[Mg^{2+}]_o = 7.2$ mM). High $[Mg^{2+}]_o$ is known to cause a complete suppression of any activated $Mg^{2+}$-sensitive current [15].

Figure 3 shows the whole-cell currents and action potentials measured in the cells dialyzed with either 0.8-mM $[Mg^{2+}]_i$ (Figure 3A,C,E) or with 0-mM $[Mg^{2+}]_i$ (Figure 3B,D,F). In these two groups of cells, there was no difference in the resting membrane potentials, which were also not changed by raising $[Mg^{2+}]_o$ from 0.9 mM to 7.2 mM (for 0.8 mM $[Mg^{2+}]_i$, the resting membrane potential: $-79.9 \pm 2.6$ mV in the control vs. $-81.0 \pm 2.1$ mV in high $[Mg^{2+}]_o$; for 0 mM $[Mg^{2+}]_i$: $-78.4 \pm 2.8$ mV in the control vs. $-77.4 \pm 3.7$ mV in high $[Mg^{2+}]_o$, $p = 0.308$, ANOVA; $n = 10$).
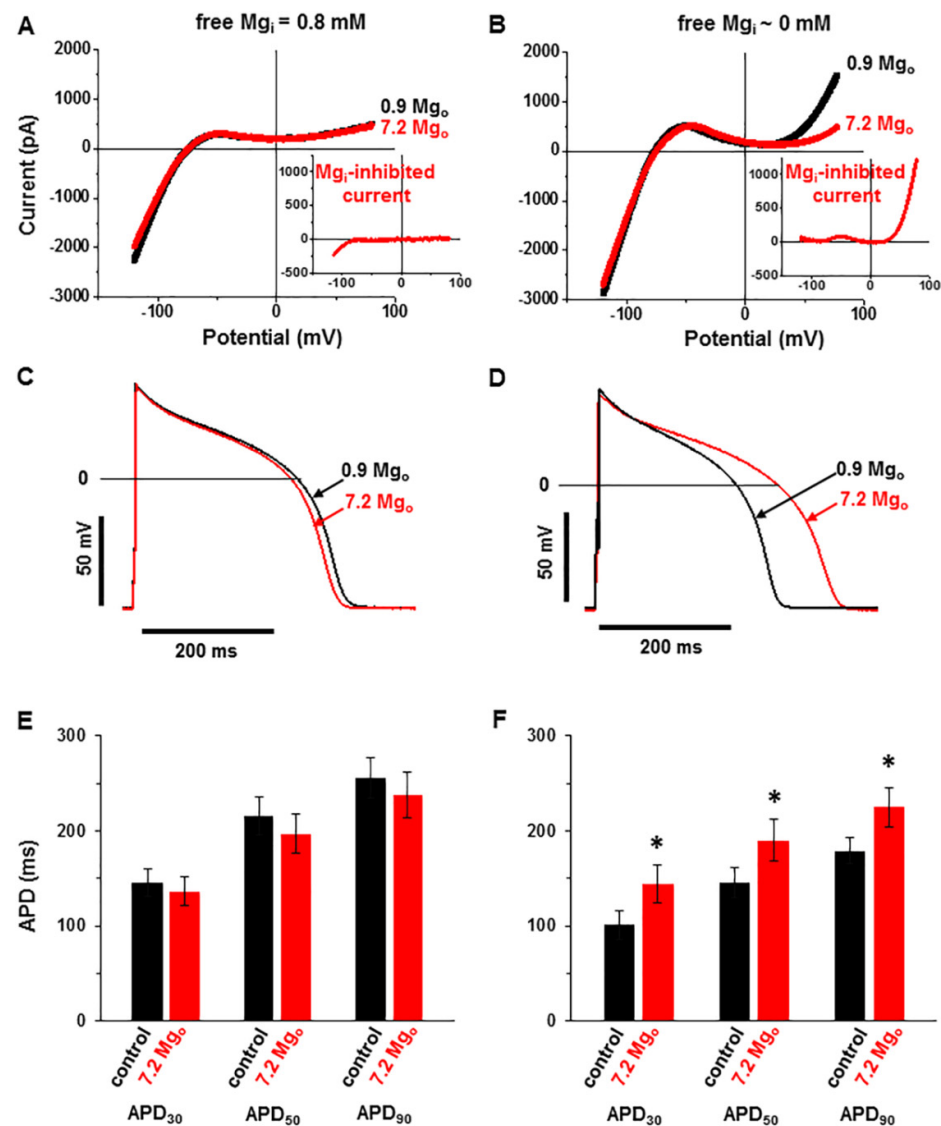
**Figure 3.** Effect of $Mg^{2+}$-sensitive current activation on the action potential. (**A**,**B**) Whole-cell currents obtained by voltage ramps in cells dialyzed with 0.8-mM $[Mg^{2+}]_i$ (**A**) or 0-mM $[Mg^{2+}]_i$ (**B**) and superfused with extracellular solutions containing 0.9-mM $[Mg^{2+}]_o$ or 7.2-mM $[Mg^{2+}]_o$. Insets: the $[Mg^{2+}]_o$-sensitive currents calculated as the differences between currents in the presence of 0.9-mM $[Mg^{2+}]_o$ and those in 7.2-mM $[Mg^{2+}]_o$. Notice the outward-rectifying $[Mg^{2+}]_o$-sensitive current in the cell dialyzed with 0-mM $[Mg^{2+}]_i$. (**C**–**F**) The action potentials in the same cells as above, and the summary data of the action potential durations (APD) from all the cells dialyzed with 0.8-mM $[Mg^{2+}]$ (**C**,**E**) or 0-mM $[Mg^{2+}]$ (**D**,**F**) and the effect of raising the $[Mg^{2+}]_o$ from 0.9 mM (black) to 7.2 mM (red). The APD was measured at 30%, 50%, and 90% repolarization (APD$_{30}$, APD$_{50}$, and APD$_{90}$, respectively). Notice the lengthening of the APD by high $[Mg^{2+}]_o$ in the cells dialyzed with low intracellular $[Mg^{2+}]$. Pacing frequency: 1 Hz. * $p < 0.05$ for 7.2-mM vs. 0.9-mM $[Mg^{2+}]_o$. $n = 9$ for the cells dialyzed with 0.8-mM $[Mg^{2+}]_i$; $n = 10$ for the cells dialyzed with 0-mM $[Mg^{2+}]_i$.

Figure 3A,B illustrates the membrane currents recorded under a voltage clamp during a descending ramp, following a preceding depolarizing ramp meant to inactivate the voltage-dependent $Na^+$- and $Ca^{2+}$ currents (see Methods). The experiments were performed at 36 °C using $K^+$-containing intra- and extracellular solutions. In cells dialyzed with physiological levels of $[Mg^{2+}]_i$ (0.8 mM; Figure 3A), the current–voltage relationship was characterized by a large inward current, consistent with the presence of the inward rectifier $K^+$ current ($I_{K1}$) at potentials negative to −75 mV, and the current–voltage relationship was relatively flat at more positive potentials. Raising $[Mg^{2+}]_o$ to 7.2 mM did not affect the current–voltage relationship, indicating that the high $[Mg^{2+}]_o$ did not affect the $I_{K1}$ and that no other $Mg^{2+}$-sensitive current was present (Figure 3A, inset). In the cells dialyzed with $Mg^{2+}$-free solution (0 mM $[Mg^{2+}]_i$; Figure 3B), the current-voltage relationship was characterized by the presence of $I_{K1}$ but also showed an outward rectifying current at positive potentials. The outward rectifying component was suppressed by raising $[Mg^{2+}]_o$ to 7.2 mM, indicating the presence of a $Mg^{2+}$-sensitive current. This $[Mg^{2+}]_o$-sensitive current, calculated as the difference in the current–voltage relationships between the two conditions with different $[Mg^{2+}]_o$, displays outward-rectifying properties similar to those of the TRPM6 and TRPM7 currents (Figure 3B, inset).

After recording membrane currents under a voltage clamp, we switched to the current clamp mode to record the action potentials in the same cells. Pig cardiomyocytes offer an experimental advantage when studying factors that affect the action potential, since channels carrying the transient outward $K^+$ current ($I_{to}$) are not expressed in this species [25,26]. Under the control conditions, with 0.9 mM $[Mg^{2+}]_o$, the action potentials were generally shorter in cells dialyzed with $Mg^{2+}$-free internal solution (compare Figure 3C,E vs. Figure 3D,F). In the cells dialyzed with physiological $[Mg^{2+}]_i$, raising $[Mg^{2+}]_o$ to 7.2 mM did not change the action potential durations during the stimulation at 1 Hz (APD; $APD_{30}$: 145.5 ± 14.5 ms vs. 136.5 ± 15.1 ms, $APD_{50}$: 216.6 ± 19.6 ms vs. 196.6 ± 21 ms, and $APD_{90}$: 238 ± 48 ms vs. 231 ± 46 ms in high $[Mg^{2+}]_o$ vs. in the control; $p > 0.05$, paired $t$-test; $n = 9$; Figure 3E). In contrast, in cells dialyzed with $Mg^{2+}$-free internal solution, raising $[Mg^{2+}]_o$ to 7.2 mM, caused a marked prolongation of the APD ($APD_{30}$: from 100.4 ± 14.8 ms to 143.6 ± 19.9 ms, $APD_{50}$: from 145.6 ± 16.1 ms to 189.8 ± 22.4 ms, and $APD_{90}$: from 178.9 ± 14.2 ms to 225.2 ± 21.3 ms; $p < 0.05$, paired $t$-test; $n = 10$; Figure 3F). Taken together, these results show that the cardiac action potential is modulated by an outward-rectifying current activated by dialysis with zero $[Mg^{2+}]_i$ and suppressed by high $[Mg^{2+}]_o$. Furthermore, given that this current was absent in the cells dialyzed with 0.8 mM $[Mg^{2+}]_i$, it is likely due to TRPM7 or/and TRPM6.

### 2.3. Effects of High Extracellular $[Mg^{2+}]$ on $I_{Ca-L}$ and $I_K$

Considering that the changes in the action potential produced by high $[Mg^{2+}]_o$ mainly affected the plateau and repolarization phases, we also examined the effect of $[Mg^{2+}]_o$ on other currents that play a role during these phases, such as the L-type $Ca^{2+}$ current ($I_{Ca-L}$) and the delayed rectifier $K^+$ current ($I_K$). The analysis was done in cells dialyzed with 0.8-mM $[Mg^{2+}]_i$ to inhibit the $Mg^{2+}$-sensitive currents. For the measurements of $I_K$, $K^+$-containing intracellular and extracellular solutions were used, and nifedipine (25 μM) was included in the external solution, whereas, for the measurements of $I_{Ca-L}$, $K^+$ was replaced by $Cs^+$ in the external and pipette solutions, and 10-mM BAPTA was used in the pipette solution instead of EGTA. Figure 4A shows the bidirectional effect of the $[Mg^{2+}]_o$ alteration on $I_{Ca-L}$. Where lowering the $[Mg^{2+}]_o$ by 10-fold to 0.09 mM reversibly increased the amplitude of $I_{Ca-L}$ continuously monitored at 0 mV ($I_{Ca-L}$ measured at the peak level: from −5.4 ± 0.43 pA/pF to −6.5 ± 0.41 pA/pF; $p < 0.05$, paired $t$-test; $n = 8$; Figure 4B), raising the $[Mg^{2+}]_o$ to 7.2 mM reversibly decreased the amplitude of $I_{Ca-L}$ (peak $I_{Ca-L}$: from −4.8 ± 0. 39pA/pF to −2.2 ± 0.17 pA/pF; $p < 0.001$, paired $t$-test; $n = 13$; Figure 4B; see reference [27]). As expected, the $I_K$ blockers E4031 and HMR1556 had no effect on the $I_{Ca-L}$ (Figure 4A). When wanting to test the consequence of an eventual modulation of the $I_{Ca-L}$ by extracellular $Mg^{2+}$, we kept E4031 constantly from the beginning of the experiment. The

$I_{Ca-L}$–voltage relationships (see Figure 4A, inset) indicate that the $[Mg^{2+}]_o$ changes shifted the activation curve of $I_{Ca-L}$ (to more negative potentials upon lowering the $[Mg^{2+}]_o$ and to more positive potentials upon raising $[Mg^{2+}]_o$; see reference [27]).
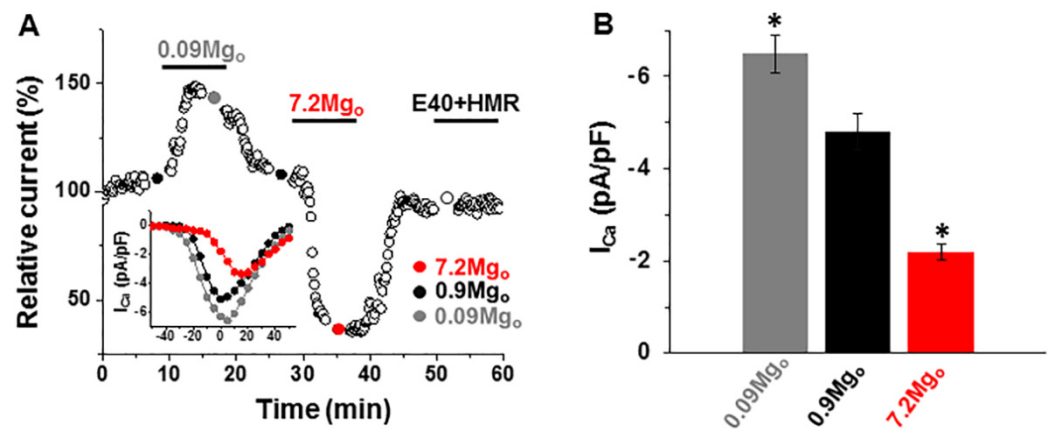


**Figure 4.** Effect of changing the external $[Mg^{2+}]$ on the L-type $Ca^{2+}$ currents ($I_{Ca-L}$). (**A**) Time diary of the amplitude of the L-type $Ca^{2+}$ currents obtained by using depolarizing steps for various potentials in a cell dialyzed with 0.8-mM $[Mg^{2+}]$ and superfused with extracellular solutions containing 0.09-mM, 0.9-mM, or 7.2-mM $[Mg^{2+}]$. Notice the increase vs. suppression of the $I_{Ca-L}$ amplitude by low vs. high $[Mg^{2+}]_o$ and the lack of effect of the $I_K$ inhibitors (E4031/HMR1556). Bottom inset: The current–voltage relations obtained by the depolarizing steps to the potentials ranging from $-50$ mV to $+50$ mV in the same cell. (**B**) Summary data of the peak $I_{Ca-L}$ amplitude and the effects of lowering and raising the $[Mg^{2+}]_o$. * $p < 0.05$ vs. 0.9-mM $[Mg^{2+}]_o$ ($n = 8$–13).

Figure 5 shows that raising $[Mg^{2+}]_o$ also decreased the magnitude of the total $I_K$ (Figure 5A at +30 mV to +50 mV $p < 0.05$ for 7.2-mM $[Mg^{2+}]_o$ vs. the control, paired *t*-test; $n = 4$) and only mildly shifted the activation curve to the right (voltage at the half-maximal current $V_{0.5}$: from $\approx -6$ mV to $\approx -2$ mV; $n = 4$; Figure 5B).
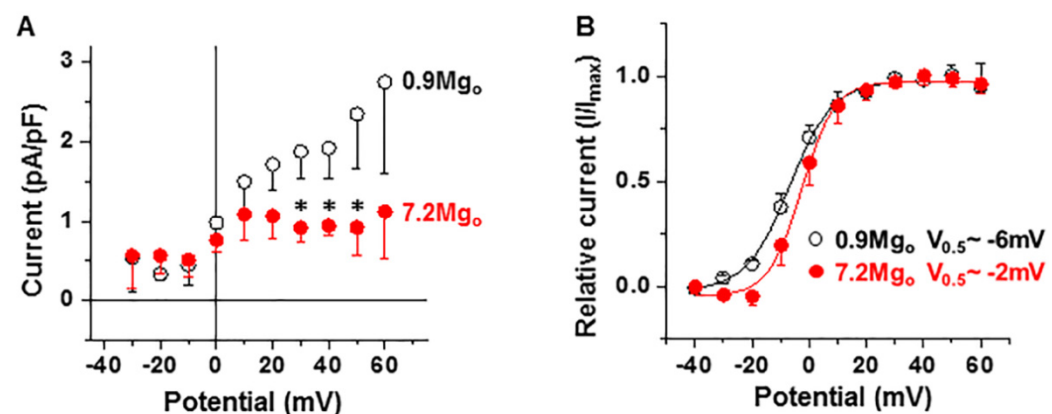


**Figure 5.** Effect of an increase of extracellular $[Mg^{2+}]$ on the total $I_K$. (**A**) The current–voltage relationship of the fully activated $I_K$ and the effect of raising the $[Mg^{2+}]_o$. Notice the suppression of $I_K$ by high $[Mg^{2+}]_o$. * $p < 0.05$ ($n = 4$). (**B**) Activation curves of $I_K$ calculated from the tail currents ($n = 4$).

Since high $[Mg^{2+}]_o$ did not change the APD in cells dialyzed with 0.8-mM $[Mg^{2+}]_i$ (see Figure 3C,E), it is possible that there are two opposing and counterbalancing effects of high $[Mg^{2+}]_o$ on the $I_{Ca-L}$ and $I_K$. To test for this possibility, we applied high $[Mg^{2+}]_o$ on cells in which the $I_K$ was partly blocked to offset such a balance. We initially performed preliminary tests to determine the optimum concentrations of the $I_K$ inhibitors (i.e., HMR1556 for the slow $I_K$ component $I_{Ks}$ and E 4031 for the rapid component $I_{Kr}$) effective in producing a

partial block of $I_K$ without excessively prolonging the APD (not illustrated). Figure 6A shows the typical changes in action potentials in a perforated cell, whereas the summary data from four cell are presented in Figure 6B. Under the control conditions with 0.9-mM $[Mg^{2+}]_o$, the addition of small concentrations of $I_K$ inhibitors (100-nM HMR1556 and 500-nM E4031) lengthened the APD, as expected from a decrease of the repolarizing $K^+$ current (at a pacing rate of 1 Hz, $APD_{30}$: from $134.6 \pm 28.5$ ms to $177.8 \pm 19.9$ ms, $APD_{50}$: from $192.9 \pm 20.9$ ms to $267.4 \pm 24.1$ ms, and $APD_{90}$: from $242.4 \pm 17.5$ ms to $358.0 \pm 18.3$ ms; * $p < 0.05$, except for the $APD_{30}$, for which $p > 0.05$, paired *t*-test; $n = 4$). Consistent with a decreased relative contribution of $I_K$, raising the $[Mg^{2+}]_o$ to 7.2 mM in the presence of the $I_K$ blockers decreased the APD (to $163.9 \pm 20.9$ ms, to $246.0 \pm 21.1$ ms, and to $323.5.0 \pm 15.5$ ms for $APD_{30}$, $APD_{50}$, and $APD_{90}$, respectively), indicating a predominant effect of $I_{Ca-L}$ suppression by high $[Mg^{2+}]_o$ under these conditions. Qualitatively similar results were obtained in three other cells dialyzed with 0.8-mM $[Mg^{2+}]_i$ under the ruptured cell membrane conditions (not illustrated). These results suggest that the lack of effect of raising $[Mg^{2+}]_o$ on the APD in cells dialyzed with 0.8-mM $[Mg^{2+}]_i$ reflects a balance in the effects of the decreases of both $I_{Ca-L}$ and $I_K$ on repolarization.
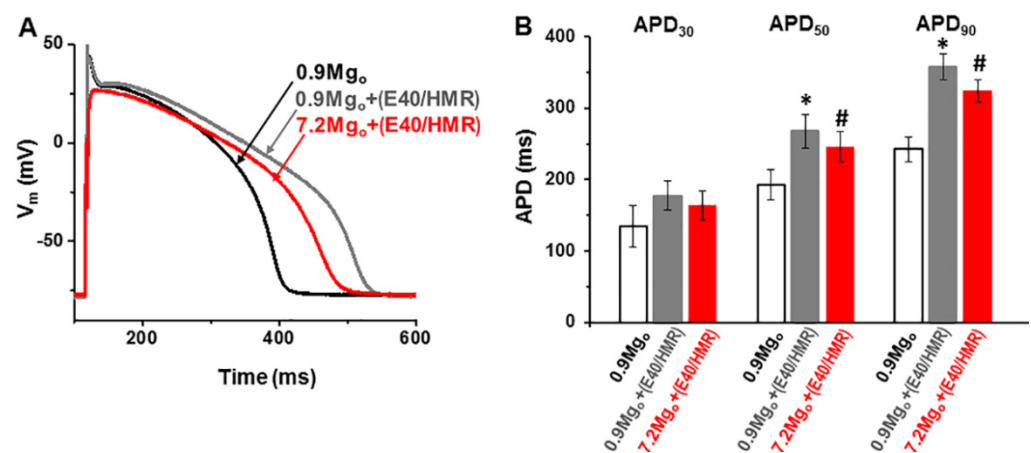


**Figure 6.** Effect of a partial $I_K$ block and high $[Mg^{2+}]_o$ on the action potential. (**A**) APs recorded at 36 °C using $K^+$-containing intra- and extracellular solutions under perforated patch conditions and initially superfused with control extracellular solutions containing 0.9-mM $[Mg^{2+}]$. A combination of HMR1556 (100 nM) and E4031 (500 nM) was then added in 0.9-mM $[Mg^{2+}]_o$ before applying 7.2-mM $[Mg^{2+}]_o$ together with the drugs. (**B**) Summary data of the AP duration (APD) at 30%, 50%, and 90% repolarization ($APD_{30}$, $APD_{50}$, and $APD_{90}$, respectively) measured under the control conditions (unshaded column) in the presence of the $I_K$ inhibitors (grey column) and in the presence of the $I_K$ inhibitors but with the $[Mg^{2+}]_o$ raised to 7.2 mM (red column). * $p < 0.05$ for the presence vs. absence of the $I_K$ inhibitors (in 0.9-mM $[Mg^{2+}]_o$). # $p < 0.05$ for 7.2-mM vs 0.9-mM $[Mg^{2+}]_o$ in the presence of the $I_K$ inhibitors ($n = 4$). Notice the shortening of the $APD_{50}$ and $APD_{90}$ by high $[Mg^{2+}]_o$ in the presence of the $I_K$ blockers.

## 3. Discussion

The results from the present study suggest the presence of TRPM6 and TRPM7 proteins in cardiac myocytes, given that immunofluorescent activity was detected in cells treated with the anti-TRPM6 or anti-TRPM7 antibody, but in contrast, no such activity was detected in the negative controls. Furthermore, the results showed that the cardiac myocyte action potential duration (APD) was shortened in the presence of a current likely due TRPM6 or TRPM7 in that it was activated by dialysis with low $[Mg^{2+}]_i$, was absent in cells dialyzed with 0.8-mM $[Mg^{2+}]_i$ and was suppressed by high $[Mg^{2+}]_o$. Thus, the results are consistent with our previous proposal that the $Mg^{2+}$-sensitive channels in the heart are likely due to TRPM6 and/or TRPM7 proteins [15] and with a possible role of the cardiac $Mg^{2+}$-sensitive channels in modulating the electrical activity.

### 3.1. Molecular Candidate for $Mg^{2+}$-Sensitive Channels

Many TRP proteins form nonselective cation channels and are, therefore, the molecular candidates for similar native channels [28]. In determining the involvement of TRPs expressed in the heart, the inhibition by $Mg^{2+}_i$ is a key distinguishing feature. For the TRPC4/C5 channels, $Mg^{2+}_i$ causes a voltage-dependent partial block of the outward currents and results in a doubly rectifying current–voltage relationship [29,30]. Such a $Mg^{2+}_i$ effect on the TRPC4/C5 channels is different from the voltage-independent slow inhibition seen in the $Mg^{2+}$-sensitive channels [15,31]. Rather, the $Mg^{2+}_i$ inhibition and the biophysical characteristics of the cardiac channels [15] resemble those of the TRPM6 and TRPM7 channels [16,19]. Our detection of TRPM6 and TRPM7 proteins by immunofluorescence suggests that the channels are expressed in both the atrial and ventricular chambers. It appears that the TRPM6 and TRPM7 channel proteins were present in both the surface membrane and intracellularly. However, where exactly the proteins are located intracellularly could not be determined in the present study. Nonetheless, a novelty of the present findings is that TRPM6 was immunodetected in pig myocytes (but see Limitations of our Study below), whereas TRPM6 expression has been reported to be lacking in other studies of cardiac tissues [32]. As such, the present results suggest that TRPM6 and TRPM7 proteins are the most likely constituents of the $Mg^{2+}$-sensitive cardiac channels.

There are, however, slight differences in the divalent cation permeability profiles between the cardiac $Mg^{2+}$-sensitive channels [15] and overexpressed TRPM7 channels [16]. It is possible that, even though the core structure of the channel may be the same, different channel subunits or regulatory units may occur in the native cells. Furthermore, the TRPM7 channel activity has been shown to be altered by heteromultimeric interactions with TRPM6 [33]. Nevertheless, in order to ascertain the cardiac channel identity, further studies are still required to correlate the activity of the TRPM6 and TRPM7 proteins detected in myocytes with the $Mg^{2+}$-sensitive current.

### 3.2. Modulation of Cardiac Electrical Activity

The possible contribution of the $Mg^{2+}$-sensitive current to cardiac electrical activity is unknown. Like in other cells, nonselective cation channels contribute to the resting membrane potential in the heart [34]. These may include $Mg^{2+}$-sensitive channels. Given the small $Mg^{2+}$-sensitive inward current and the large $I_{K1}$ at a negative potential in the heart, the $Mg^{2+}$-sensitive channels would not be expected to contribute significantly to the background non-$K^+$ permeability in resting cardiomyocytes. This is consistent with our findings here, showing no effect of raising the extracellular $Mg^{2+}$ concentration on the resting membrane potential. However, in other tissues such as vascular smooth muscle, the contribution of nonselective cation channels, some of which resemble TRPM6 and TRPM7, could be more important [35,36].

Cation nonselective channels may also contribute to shaping the cardiac action potential. In atrial cells, a stretch-activated cation nonselective channel has been shown to contribute to both the resting and action potentials [37]. Since the net ion current is small during the plateau phase of the action potential, changes in the large monovalent cation effluxes through $Mg^{2+}$-sensitive channels at positive potentials may have significant effects on the action potential. Consistent with such an expectation, our present results showed that the activation of the cardiac $Mg^{2+}$-sensitive channels shortened the APD. It is unlikely that the APD shortening is due to a larger outward $I_{K1}$ following the removal of the $Mg^{2+}_i$ block in low $[Mg^{2+}]_i$ conditions, since endogenous polyamines would still continue to provide a sufficient block of the outward $I_{K1}$ [38] and since high $Mg^{2+}_o$ suppressed the outward current while having no effect on the inward currents. Our results suggest that there is practically no contribution of TRPM6 and TRPM7 currents to the AP when $[Mg^{2+}]_i$ is at the physiological levels. This result is consistent with a lack of changed currents through mutant TRPM7 channels expressed in cultured cardiomyocytes on the action potentials measured in such cells [39].

### 3.3. Clinical Implications

A key question concerns the conditions under which the $Mg^{2+}$-sensitive channels may contribute to cardiac electrical activity. Under the physiological conditions (free $[Mg^{2+}]_i$ 0.8 mM; $IC_{50} \approx 0.25$ mM; [15,31]), the channels are expected to be substantially inhibited by $Mg^{2+}_i$. However, the $Mg^{2+}$-sensitive current may contribute to APD if the sensitivity to $[Mg^{2+}]_i$ is decreased by regulatory processes or channel mutations or if $[Mg^{2+}]_i$ is decreased to low levels by disease conditions such as chronic hypomagnesaemia. Indeed, the TRPM7 and related native channels show constitutive activity, some of it in cells where the intracellular ion composition (including $[Mg^{2+}]_i$) remains relatively unperturbed [16,18,40], suggesting the presence of other regulatory processes. In cardiac cells, besides $[Mg^{2+}]_i$, the $Mg^{2+}$-sensitive channels are also regulated by factors such as the pH change and membrane phospholipid metabolism [14,15,41], but it is still not known whether such regulatory processes can induce the constitutive activity of the channels. In the present study, we show that the expression of the TRPM6 and TRPM7 channels is modulated by incubation in divalent cation-free extracellular conditions. Thus, the contributions of the $Mg^{2+}$-sensitive current to the AP may vary depending on the status of the extracellular divalent cation homeostasis.

Earlier studies demonstrated TRPM7 activation by free oxygen radicals during prolonged neuronal ischemia [42]. To date, the functional role of TRPM7 and especially that of TRPM6 are less clearly understood in heart cardiomyocytes compared to vascular smooth muscle cells [43], neurons, or other cell types [44,45]. The molecular and electrophysiological characterizations of TRPM7 in the heart have focused predominantly on cardiac fibroblasts. TRPM7 activation in human atrial fibroblasts leads to fibrogenesis and atrial fibrillation [46]. Additionally, the variability of the TRPM7 current density in human right atrial cardiomyocytes is related to the clinical history, being higher in disease conditions such as atrial fibrillation [47,48] and in ischemic heart disease [48]. Very recently, we also demonstrated the presence and co-expression of both TRPM6 and TRPM7 in cardiomyocytes from the four chamber walls of the human heart [22] and also showed that ischemic heart disease may increase their expression, suggesting that chanzymes are involved in the pathophysiology of the disease.

### 3.4. Limitations of the Study

Given the current uncertainty about the detection of TRPM6 in cardiac cells, it is important to examine how convincing the evidence is for the presence of TRPM6 in our study.

The present study relied on immunostaining to detect the presence of TRPM7 and TRPM6. Previous studies have demonstrated limitations of antibody staining methods to determine the expression of TRP channels (e.g., see [49]). The specificity of the commercial antibodies used in our study was not directly tested, e.g., using blocking peptides or using cells lines in which the TRPM7 and TRPM6 genes were knocked out, silenced or overexpressed.

Our results, using swine cardiomyocytes, are in concordance to human TRPM6 and TRPM7 immunodetected fluorescence distribution, which also suggested both ion channel expression in the walls of all cardiac chambers [22]. In that study RT-PCR confirmed the presence of mRNA for both TRPM7 and TRPM6, hence supporting the immunostaining data, but the interpretation of RT-PCR also has limitations due to possible contamination by non-cardiomyocyte cells. We used on pig myocytes the same antibodies as in that study. Although these antibodies are recognized to work on human proteins, a key limitation of the present study is that there is no previous evidence of their specificity in pig cells and there are no readily available pig-specific TRPM6 antibodies in the market. Given that there is a great amount of antibody recognition between human- and pig epitopes in cardiac tissue [50], we used the same TRPM6 antibody (designed for human, mouse, and rat), which being polyclonal, would also be able to bind to epitopes in other species.

Although TRPM6 was detected in pig cardiomyocytes but not in negative controls, the specificity of the antibody in pig still requires verification in future studies.

An important limitation of the electrophysiological study is that there are, as yet, no known specific pharmacological blockers available for $Mg^{2+}$-sensitive- and related channels. Presently, we used the block by $Mg^{2+}_o$ as an extracellular tool to isolate the $Mg^{2+}$-sensitive current. There was therefore a possible confounding issue in that $Mg^{2+}_o$ could also suppress $I_{Ca-L}$ and $I_K$. In other studies, the $Mg^{2+}_o$ effect on $I_K$ was more prominent on tail currents during repolarization [51], and increasing $Mg^{2+}_o$ caused either a lengthening or a shortening of APD, depending on the level of $Mg^{2+}_o$ [52]. However, in the present study, the $Mg^{2+}_o$ effects on action potentials that were due to $I_{Ca-L}$ and $I_K$ seemed to balance each other out sufficiently for their effects to be isolated from those on the $Mg^{2+}$-sensitive current.

### 3.5. Conclusion

In conclusion, our results show the presence of TRPM7 and, to a certain extent, suggest that of TRPM6 proteins in pig cardiomyocytes, making these proteins the molecular candidates for cardiac $Mg^{2+}$-sensitive channels. The activation of the $Mg^{2+}$-sensitive channels shortened the cardiomyocyte APD. Although the pathophysiological conditions in which the channels are activated remain unclear, the effect of the $Mg^{2+}$-sensitive current on the APD may be important in understanding the therapeutic processes in which $Mg^{2+}$ is empirically used to treat arrhythmias, as well as in linking the changes in $Mg^{2+}$ homeostasis to other cardiac disease conditions.

### 4. Materials and Methods

We used isolated, single cardiomyocytes of a pig heart. This study was carried out in compliance with the Guide for the Care and Use of Laboratory Animals (NIH). All experiments were performed according to the European Community guiding principles and approved by the State Food and Veterinary Service of the Republic of Lithuania (No. G2-68, 21 June 2017) and by the Belgian laboratory license No. LA-1210253.

### 4.1. Cell Isolation

The methods used for the dissociation of pig cells have been described before [15,25]. In short, for electrophysiology studies, a piece of the left ventricular wall was excised, and its supplying artery was cannulated and perfused at 37 °C and at constant pressure for 30 min with an oxygenated $Ca^{2+}$-free Tyrode solution, followed by a 20- to 25-min perfusion with a $Ca^{2+}$-free Tyrode solution containing 0.1-mg mL$^{-1}$ protease (type XIV, Sigma-Aldrich, St. Louis, MO, USA) and 1.4-mg mL$^{-1}$ collagenase (type A, Boehringer-Mannheim, Mannheim, Germany). After a 15-min washing perfusion with a 0.18-mM $Ca^{2+}$ Tyrode solution, the tissue was removed from the perfusion and was cut into small pieces. The cells were dispersed by gentle mechanical agitation. $[Ca^{2+}]_o$ was raised in a stepwise manner, and the cells were stored at room temperature (21–22 °C). $Ca^{2+}$-tolerant rod-shaped ventricular myocytes with clear striations were selected for the electrophysiological studies.

For the immunofluorescence studies, the cardiomyocytes were isolated from a small tissue specimen as previously described [53]. In short, each tissue specimen (LA, RA, LV, and RV) was fine-cut in an oxygenated nominally $Ca^{2+}$-free Tyrode solution (see the composition below) supplemented with 3-mg/mL 2,3-butanedione monoxime, which was washed out 2 to 3 times before the enzyme application. The cardiac tissue chunks were transferred to a beaker with nominally $Ca^{2+}$-free Tyrode solution supplemented with 1-mg/mL bovine serum albumin (BSA), 1-mg/mL collagenase (215 U/mg, type 2; Worthington Biochemical Corporation, Lakewood, NJ, USA), and 0.5-mg/mL protease (7–14 U/mg, type XXIV; Sigma-Aldrich, St. Louis, MO, USA) and continuously bubbled with 100% $O_2$. After 30 min of shaking in a water bath at 37 °C, the solution with both enzymes was replaced by fresh solution containing only collagenase (1 mg/mL) and shaken until cardiomyocytes appeared in the aliquots obtained from the mixture. When

the yield appeared to be optimal, the leftovers of the tissue chunks were resuspended in nominally $Ca^{2+}$-free Tyrode and gently subjected to trituration by suction with a pipette. The cell suspension was filtered, centrifuged, and washed 2 to 3 times either with normal (divalent cation-containing) or with divalent cation-free Tyrode solution and stored at room temperature.

### 4.2. Electrophysiology

Whole-cell currents were recorded under a voltage clamp, and the action potentials were recorded under a current clamp at 36 °C within 4 h after cell isolation. The membrane currents of interest were measured using 2-s descending voltage ramps from +80 mV to −120 mV applied every 10 s after a 600-ms pre-step at 0 mV from a holding potential of −80 mV, designed to inactivate the voltage-dependent $Na^+$ and L-type $Ca^{2+}$ currents. For measuring the L-type $Ca^{2+}$ currents ($I_{Ca-L}$), 400-ms depolarizations to various potentials were given after a 400-ms pre-step at −40 mV, designed to inactivate the voltage-dependent $Na^+$ current. The total delayed rectifier $K^+$ currents $I_K$ were measured using voltage steps from a holding potential of −40 mV to various positive potentials, and the tail currents were then measured upon reverting to −50 mV. The action potentials were measured by stimulating with a 2-ms rectangular pulse at a frequency of 1 Hz. The action potential duration (APD) was measured at 30% ($APD_{30}$), 50% ($APD_{50}$), and 90% ($APD_{90}$) repolarization. The current and voltage protocols were generated and data recorded online using the Axopatch 200B amplifier and pClamp 8.1 software via the Digidata 1322A acquisition system (Axon instruments, Union City, CA, USA).

### 4.3. Immunofluorescence

Enzymatically dissociated cardiomyocytes were allowed to settle on the bottom of 8-chamber slides. The cells were permeabilized and incubated with primary rabbit polyclonal anti-TRPM7 (#ACC-047; Alomone Labs, Jerusalem, Israel) or rabbit polyclonal anti-TRPM6 antibody (#ACC-046; Alomone Labs, Jerusalem, Israel) diluted (1:200) in PBS containing 3% BSA in blocking buffer overnight at 4 °C. The TRPM6 and TRPM7 antibodies were obtained from the same company in order to minimize the possibility of cross-reactivity during immunolabeling. For the negative controls, incubation with the primary antibody was omitted to check for nonspecific binding of the secondary antibody. The cells were incubated for 1 h with a fluorescently labeled secondary antibody (donkey anti-rabbit IgG; Alexa Fluor® 488 conjugate; A21206, Invitrogen, Thermo Fisher Scientific, Rockford, IL, USA; dilution 1:200) co-stained (for 20 min) with Phalloidin-Alexa Fluor® 546 (A22283, Invitrogen, Thermo Fisher Scientific, Waltham, MA, USA; dilution 1:100) and with Hoechst 33342 (B2261, Sigma-Aldrich, St. Louis, MO, USA; for 10 min) for labeling of the F-actin cytoskeleton and of the nucleus, respectively. Cardiomyocytes were visualized under a confocal laser scanning microscope (Olympus BX61, Olympus Corporation, Tokyo, Japan) from which images were taken using the same scanning parameters for both the TRPM7 and TRPM6 proteins in all the cardiomyocyte preparations.

### 4.4. Solutions and Drugs

The standard Tyrode solution used during cell dissociation contained (in mM): 135 NaCl, 5.4 KCl, 0.9 $MgCl_2$, 1.8 $CaCl_2$, 0.33 $NaH_2PO_4$, 10 HEPES, and 10 glucose; the pH was adjusted to 7.4 with NaOH. During the patch clamp measurements, the cells were superfused with a solution of similar composition, except that, when necessary, $K^+$ was replaced by $Cs^+$, and the $Mg^{2+}$ levels were changed. The standard pipette solution was contained (in mM): 155 KCl, 5.5 $MgCl_2$, 5 $Na_2ATP$, 1 EGTA, 0.1 $Na_2GTP$, and 5 HEPES (pH 7.25; adjusted with KOH) and was modified by changing the levels of $Mg^{2+}$, by replacing $K^+$ with $Cs^+$, or by substituting EGTA with BAPTA. The phosphate-buffered saline (PBS) used in immunofluorescence contained (in mM): 155.2 NaCl, 2.71 $Na_2HPO_4 \cdot 2H_2O$, and 1.54 $KH_2PO_4$ (pH 7.4; adjusted with NaOH).

HMR1556 was from Aventis Pharma, Frankfurt Am Main, Germany, and E-4031 was from Tocris, Bristol, UK. All the other drugs or chemicals were from Sigma-Aldrich (Bornem, Belgium) or Merck (Darmstadt, Germany). Nifedipine was prepared as a stock solution in ethanol and was protected from light, whereas HMR1556 was prepared in dimethyl sulfoxide (DMSO). All the other chemicals were dissolved in water.

*4.5. Data and Statistical Analyses*

An electrophysiology data analysis was performed using Clampfit 8.2 (Axon Instruments, Union City, CA, USA) and Origin 7 (Microcal, Northampton, MA, USA).

The distribution of the immunofluorescence was analyzed using the Olympus Fluoview FV1000 (Olympus Corporation, Tokyo, Japan) and ImageJ software. Sixty-times magnifying ($60\times$) of the oil immersion objectives were utilized for all the acquisitions. The images were presented as stacks of 8–10 slices at a fixed intensity. The cardiomyocyte area (pixels) and fluorescence intensity were measured in stacks using Imaris software (Bitplane AG, Zurich, Switzerland). The immunodetected TRPM6 and TRPM7 protein levels were calculated by the formula: fluorescence intensity $\times$ 1000/cell area. In order to reduce the effect on any statistical confounder, the same parameters for fluorescence intensity detection (image acquisition control and spectral settings, etc.) were always applied. In addition, the immunofluorescence reading was blinded, as the conditions used to keep the cells were unknown to the person performing the reading.

The average data were presented as the mean $\pm$ standard error of the mean (S.E.M) or box plots, with *n* indicating the number of cells studied under each condition. The means were compared using the two-tailed Student's *t*-test, whereas differences among the multiple groups were evaluated using an analysis of variance (ANOVA). $p \leq 0.05$ was taken as the threshold for statistical significance.

**Author Contributions:** Conceptualization, A.G., K.M., and R.M.; investigation, A.G., I.A., B.M.I., F.E., and R.M.; formal analysis, A.G., I.A., B.M.I., F.E., and R.M.; validation, A.G., K.M., and R.M.; and writing—review and editing A.G., K.M., and R.M. All authors have read and agreed to the published version of the manuscript.

**Institutional Review Board Statement:** All experiments were performed according to the European Community guiding principles and approved by the State Food and Veterinary Service of the Republic of Lithuania (No. G2-68, 21 June 2017) and by the Belgian laboratory license No. LA-1210253.

**Informed Consent Statement:** Not applicable.

**Conflicts of Interest:** The authors declare no conflict of interest.

## References

1. DiFrancesco, D. Serious workings of the funny current. *Prog. Biophys. Mol. Biol.* **2006**, *90*, 13–25. [CrossRef]
2. Falcón, D.; Galeano-Otero, I.; Calderón-Sánchez, E.; Del Toro, R.; Martin-Bornez, M.; Rosado, J.A.; Hmadcha, A.; Smani, T. TRP channels: Current perspectives in the adverse cardiac remodeling. *Front. Physiol.* **2019**, *10*, 159. [CrossRef] [PubMed]
3. Hof, T.; Chaigne, S.; Récalde, A.; Sallé, L.; Brette, F.; Guinamard, R. Transient receptor potential channels in cardiac health and disease. *Nat. Rev. Cardiol.* **2019**, *16*, 344–360. [CrossRef] [PubMed]
4. Hu, Y.; Li, Q.; Kurahara, L.H.; Shioi, N.; Hiraishi, K.; Fujita, T.; Zhu, X.; Inoue, R. An Arrhythmic Mutation E7K Facilitates TRPM4 Channel Activation via Enhanced PIP2 Interaction. *Cells* **2021**, *10*, 983. [CrossRef]
5. Feng, J.; Zong, P.; Yan, J.; Yue, Z.; Li, X.; Smith, C.; Ai, X.; Yue, L. Upregulation of transient receptor potential melastatin 4 (TRPM4) in ventricular fibroblasts from heart failure patients. *Pflügers Arch.* **2021**, *473*, 521–531. [CrossRef] [PubMed]
6. Seth, M.; Zhang, Z.S.; Mao, L.; Graham, V.; Burch, J.; Stiber, J.; Tsiokas, L.; Winn, M.; Abramowitz, J.; Rockman, H.A.; et al. TRPC1 channels are critical for hypertrophic signaling in the heart. *Circ. Res.* **2009**, *105*, 1023–1030. [CrossRef]

7.  Alvarez, J.; Coulombe, A.; Cazorla, O.; Ugur, M.; Rauzier, J.M.; Magyar, J.; Mathieu, E.L.; Boulay, G.; Souto, R.; Bideaux, P.; et al. ATP/UTP activate cation-permeable channels with TRPC3/7 properties in rat cardiomyocytes. *Am. J. Physiol. Heart Circ. Physiol.* **2008**, *295*, H21–H28. [CrossRef] [PubMed]

8.  Onohara, N.; Nishida, M.; Inoue, R.; Kobayashi, H.; Sumimoto, H.; Sato, Y.; Mori, Y.; Nagao, T.; Kurose, H. TRPC3 and TRPC6 are essential for angiotensin II-induced cardiac hypertrophy. *EMBO J.* **2006**, *25*, 5305–5316. [CrossRef]

9.  Chaigne, S.; Cardouat, G.; Louradour, J.; Vaillant, F.; Charron, S.; Sacher, F.; Ducret, T.; Guinamard, R.; Vigmond, E.; Hof, T. Transient receptor potential vanilloid 4 channel participates in mouse ventricular electrical activity. *Am. J. Physiol. Heart Circ. Physiol.* **2021**, *320*, H1156–H1169. [CrossRef]

10. Guinamard, R.; Chatelier, A.; Demion, M.; Potreau, D.; Patri, S.; Rahmati, M.; Bois, P. Functional characterization of a $Ca^{2+}$-activated non-selective cation channel in human atrial cardiomyocytes. *J. Physiol.* **2004**, *558*, 75–83. [CrossRef]

11. Sah, R.; Mesirca, P.; Van den Boogert, M.; Rosen, J.; Mably, J.; Mangoni, M.E.; Clapham, D.E. Ion channel-kinase TRPM7 is required for maintaining cardiac automaticity. *Proc. Natl. Acad. Sci. USA* **2013**, *110*, E3037–E3046. [CrossRef] [PubMed]

12. Sah, R.; Mesirca, P.; Mason, X.; Gibson, W.; Bates-Withers, C.; Van den Boogert, M.; Chaudhuri, D.; Pu, W.T.; Mangoni, M.E.; Clapham, D.E. Timing of myocardial Trpm7 deletion during cardiogenesis variably disrupts adult ventricular function, conduction, and repolarization. *Circulation* **2013**, *128*, 101–114. [CrossRef] [PubMed]

13. Volk, T.; Schwoerer, A.P.; Thiessen, S.; Schultz, J.H.; Ehmke, H. A polycystin-2-like large conductance cation channel in rat left ventricular myocytes. *Cardiovasc. Res.* **2003**, *58*, 76–88. [CrossRef]

14. Gwanyanya, A.; Sipido, K.R.; Vereecke, J.; Mubagwa, K. ATP and PIP2 dependence of the magnesium-inhibited, TRPM7-like cation channel in cardiac myocytes. *Am. J. Physiol. Cell Physiol.* **2006**, *291*, C627–C635. [CrossRef]

15. Gwanyanya, A.; Amuzescu, B.; Zakharov, S.I.; Macianskiene, R.; Sipido, K.R.; Bolotina, V.M.; Vereecke, J.; Mubagwa, K. Magnesium-inhibited, TRPM6/7-like channel in cardiac myocytes: Permeation of divalent cations and pH-mediated regulation. *J. Physiol.* **2004**, *559*, 761–776. [CrossRef]

16. Monteilh-Zoller, M.K.; Hermosura, M.C.; Nadler, M.J.; Scharenberg, A.M.; Penner, R.; Fleig, A. TRPM7 provides an ion channel mechanism for cellular entry of trace metal ions. *J. Gen. Physiol.* **2003**, *121*, 49–60. [CrossRef]

17. Nadler, M.J.; Hermosura, M.C.; Inabe, K.; Perraud, A.L.; Zhu, Q.; Stokes, A.J.; Kurosaki, T.; Kinet, J.P.; Penner, R.; Scharenberg, A.M.; et al. LTRPC7 is a Mg.ATP-regulated divalent cation channel required for cell viability. *Nature* **2001**, *411*, 590–595. [CrossRef]

18. Schmitz, C.; Perraud, A.L.; Johnson, C.O.; Inabe, K.; Smith, M.K.; Penner, R.; Kurosaki, T.; Fleig, A.; Scharenberg, A.M. Regulation of vertebrate cellular $Mg^{2+}$ homeostasis by TRPM7. *Cell* **2003**, *114*, 191–200. [CrossRef]

19. Voets, T.; Nilius, B.; Hoefs, S.; van der Kemp, A.W.; Droogmans, G.; Bindels, R.J.; Hoenderop, J.G. TRPM6 forms the $Mg^{2+}$ influx channel involved in intestinal and renal $Mg^{2+}$ absorption. *J. Biol. Chem.* **2004**, *279*, 19–25. [CrossRef]

20. Fleig, A.; Chubanov, V. TRPM7. *Handb. Exp. Pharmacol.* **2014**, *222*, 521–546. [PubMed]

21. Zhang, Y.J.; Ma, N.; Su, F.; Liu, H.; Mei, J. Increased TRPM6 expression in atrial fibrillation patients contribute to atrial fibrosis. *Exp. Mol. Pathol.* **2015**, *98*, 486–490. [CrossRef]

22. Andriulė, I.; Pangonytė, D.; Almanaitytė, M.; Patamsytė, V.; Kuprytė, M.; Karčiauskas, D.; Mubagwa, K.; Mačianskienė, R. Evidence for the expression of TRPM6 and TRPM7 in cardiomyocytes from all four chamber walls of the human heart. *Sci. Rep.* **2021**, *11*, 1–14.

23. Tashiro, M.; Inoue, H.; Konishi, M. Physiological pathway of magnesium influx in rat ventricular myocytes. *Biophys. J.* **2014**, *107*, 2049–2058. [CrossRef]

24. Gräbner, W.; Pfitzer, P. Number of nuclei in isolated myocardial cells of pigs. *Virchows Arch. B Cell Pathol.* **1974**, *15*, 279–294.

25. Macianskiene, R.; Moccia, F.; Sipido, K.R.; Flameng, W.; Mubagwa, K. Channels involved in transient currents unmasked by removal of extracellular calcium in cardiac cells. *Am. J. Physiol. Heart Circ. Physiol.* **2002**, *282*, H1879–H1888. [CrossRef] [PubMed]

26. Li, G.R.; Du, X.L.; Siow, Y.L.; O, K.; Tse, H.F.; Lau, C.P. Calcium-activated transient outward chloride current and phase 1 repolarization of swine ventricular action potential. *Cardiovasc. Res.* **2003**, *58*, 89–98. [CrossRef]

27. Hartzell, H.C.; White, R.E. Effects of magnesium on inactivation of the voltage-gated calcium current in cardiac myocytes. *J. Gen. Physiol.* **1989**, *94*, 745–767. [CrossRef]

28. Clapham, D.E. TRP channels as cellular sensors. *Nature* **2003**, *426*, 517–524. [CrossRef] [PubMed]

29. Obukhov, A.G.; Nowycky, M.C. A cytosolic residue mediates $Mg^{2+}$ block and regulates inward current amplitude of a transient receptor potential channel. *J. Neurosci.* **2005**, *25*, 1234–1239. [CrossRef] [PubMed]

30. Schaefer, M.; Plant, T.D.; Obukhov, A.G.; Hofmann, T.; Gudermann, T.; Schultz, G. Receptor-mediated regulation of the nonselective cation channels TRPC4 and TRPC5. *J. Biol. Chem.* **2000**, *275*, 17517–17526. [CrossRef] [PubMed]

31. Zakharov, S.I.; Smani, T.; Leno, E.; Macianskiene, R.; Mubagwa, K.; Bolotina, V.M. Monovalent cation (MC) current in cardiac and smooth muscle cells: Regulation by intracellular $Mg^{2+}$ and inhibition by polycations. *Br. J. Pharmacol.* **2003**, *138*, 234–244. [CrossRef]

32. Schlingmann, K.P.; Weber, S.; Peters, M.; Niemann-Nejsum, L.; Vitzthum, H.; Klingel, K.; Kratz, M.; Haddad, E.; Ristoff, E.; Dinour, D.; et al. Hypomagnesemia with secondary hypocalcemia is caused by mutations in TRPM6, a new member of the TRPM gene family. *Nat. Genet.* **2002**, *31*, 166–170. [CrossRef] [PubMed]

33. Chubanov, V.; Waldegger, S.; Mederos y Schnitzler, M.; Vitzthum, H.; Sassen, M.C.; Seyberth, H.W.; Konrad, M.; Gudermann, T. Disruption of TRPM6/TRPM7 complex formation by a mutation in the TRPM6 gene causes hypomagnesemia with secondary hypocalcemia. *Proc. Natl. Acad. Sci. USA* **2004**, *101*, 2894–2899. [CrossRef]

34. Isenberg, G. Nonselective cation channels in cardiac and smooth muscle cells. *Nonselective Cation Channels* **1993**, *66*, 247–260.

35. Zakharov, S.I.; Mongayt, D.A.; Cohen, R.A.; Bolotina, V.M. Monovalent cation and L-type Ca²⁺ channels participate in calcium paradox-like phenomenon in rabbit aortic smooth muscle cells. *J. Physiol.* **1999**, *514*, 71–81. [CrossRef] [PubMed]

36. Bae, Y.M.; Park, M.K.; Lee, S.H.; Ho, W.K.; Earm, Y.E. Contribution of Ca²⁺-activated K⁺ channels and non-selective cation channels to membrane potential of pulmonary arterial smooth muscle cells of the rabbit. *J. Physiol.* **1999**, *514*, 747–758. [CrossRef]

37. Zhang, Y.H.; Youm, J.B.; Sung, H.K.; Lee, S.H.; Ryu, S.Y.; Ho, W.K.; Earm, Y.E. Stretch-activated and background non-selective cation channels in rat atrial myocytes. *J. Physiol.* **2000**, *523*, 607–619. [CrossRef] [PubMed]

38. Lopatin, A.N.; Makhina, E.N.; Nichols, C.G. Potassium channel block by cytoplasmic polyamines as the mechanism of intrinsic rectification. *Nature* **1994**, *372*, 366–369. [CrossRef]

39. Cartwright, J.H.; Aziz, Q.; Harmer, S.C.; Thayyil, S.; Tinker, A.; Munroe, P.B. Genetic variants in TRPM7 associated with unexplained stillbirth modify ion channel function. *Hum. Mol. Genet.* **2020**, *29*, 1797–1807. [CrossRef]

40. Kozak, J.A.; Kerschbaum, H.H.; Cahalan, M.D. Distinct properties of CRAC and MIC channels in RBL cells. *J. Gen. Physiol.* **2002**, *120*, 221–235. [CrossRef]

41. Macianskiene, R.; Gwanyanya, A.; Vereecke, J.; Mubagwa, K. Inhibition of the magnesium-sensitive TRPM7-like channel in cardiac myocytes by nonhydrolysable GTP analogs: Involvement of phosphoinositide metabolism. *Cell Physiol. Biochem.* **2008**, *22*, 109–118. [CrossRef]

42. Aarts, M.; Iihara, K.; Wei, W.L.; Xiong, Z.G.; Arundine, M.; Cerwinski, W.; MacDonald, J.F.; Tymianski, M. A key role for TRPM7 channels in anoxic neuronal death. *Cell* **2003**, *115*, 863–877. [CrossRef]

43. Touyz, R. Transient receptor potential melastatin 6 and 7 channels, magnesium transport, and vascular biology: Implication in hypertension. *Am. J. Physiol. Heart Circ. Physiol.* **2008**, *294*, H1103–H1118. [CrossRef] [PubMed]

44. Sun, H.; Jackson, M.; Martin, L.; Jansen, K.; Teves, L.; Cui, H.; Kiyonaka, S.; Mori, Y.; Jones, M.; Forder, J.P.; et al. Suppression of hipocampal TRPM7 protein prevents delayed neuronal death in brain ischemia. *Nat. Neurosci.* **2009**, *12*, 1300–1307. [CrossRef] [PubMed]

45. Krapivinsky, G.; Mochita, S.; Krapivinsky, L.; Cibulsky, S.; Clapham, D. The TRPM7 ion channel function in cholinergic synaptic vesicles and affects transmitter release. *Neuron* **2006**, *52*, 485–496. [CrossRef] [PubMed]

46. Du, J.; Xie, J.; Zhang, Z.; Tsujikawa, H.; Fusco, D.; Silverman, D.; Liang, B.; Yue, L. TRPM7-mediated Ca²⁺ signals confer fibrogenesis in human atrial fibrillation. *Circ. Res.* **2010**, *106*, 992–1003. [CrossRef] [PubMed]

47. Zhang, Y.H.; Sun, H.Y.; Chen, K.H.; Du, X.L.; Liu, B.; Cheng, L.C.; Li, X.; Jin, M.W.; Li, G.R. Evidence for functional expression of TRPM7 channels in human atrial myocytes. *Basic Res. Cardiol.* **2012**, *107*, 282. [CrossRef] [PubMed]

48. Macianskiene, R.; Almanaityte, M.; Jekabsone, A.; Mubagwa, K. Modulation of human cardiac TRPM7 current by extracellular acidic pH depends upon extracellular concentrations of divalent cations. *PLoS ONE* **2017**, *12*, e0170923. [CrossRef]

49. Nilius, B.; Flockerzi, V. What do we really know and what do we need to know: Some controversies, perspectives, and surprises. *Handb. Exp. Phalmacol.* **2014**, *223*, 1239–1280.

50. Scalia, C.R.; Gendusa, R.; Basciu, M.; Riva, L.; Tusa, L.; Musarò, A.; Veronese, S.; Formenti, A.; D'Angelo, D.; Ronzio, A.G.; et al. Epitope recognition in the Human–Pig comparison model on fixed and embedded material. *J. Histochem. Cytochem.* **2015**, *63*, 805–822. [CrossRef]

51. Po, S.S.; Wang, D.W.; Johnson, J.P., Jr.; Nie, L.; Bennett, P.B. Modulation of HERG potassium channels by extracellular magnesium and quinidine. *J. Cardiovasc. Pharmacol.* **1999**, *33*, 181–185. [CrossRef] [PubMed]

52. Zhang, S.; Sawanobori, T.; Adaniya, H.; Hirano, Y.; Hiraoka, M. Dual effects of external magnesium on action potential duration in guinea pig ventricular myocytes. *Am. J. Physiol. Heart Circ. Physiol.* **1995**, *268*, H2321–H2328. [CrossRef] [PubMed]

53. Macianskiene, R.; Martisiene, I.; Zablockaite, D.; Gendviliene, V. Characterization of Mg²⁺-regulated TRPM7-like current in human atrial myocytes. *J. Biomed. Sci.* **2012**, *19*, 75. [CrossRef] [PubMed]